IEEE Access
Multidisciplinary | Rapid Review | Open Access Journal

SPECIAL SECTION ON ADVANCED COMMUNICATIONS AND NETWORKING TECHNIQUES FOR WIRELESS CONNECTED INTELLIGENT ROBOT SWARMS

Received January 23, 2020, accepted February 4, 2020, date of publication February 14, 2020, date of current version February 26, 2020.

Digital Object Identifier 10.1109/ACCESS.2020.2974002

Interleaver Design for Small-Coupling-Length Spatially Coupled Protograph LDPC-Coded BICM Systems Over Wireless Fading Channels

YUNLONG ZHAO, YI FANG, (Member, IEEE), AND ZHAOJIE YANG
School of Information Engineering, Guangdong University of Technology, Guangzhou 510006, China
State Key Laboratory of Integrated Services Networks, Xidian University, Xi'an 710126, China

Corresponding author: Yi Fang (fangyi@gdut.edu.cn)

This work was supported in part by the NSF of China under Grant 61771149, in part by the Open Research Fund of the State Key Laboratory of Integrated Services Networks under Grant ISN19-04, in part by the NSF of Guangdong Province under Grant 2019A1515011465 and Grant 2016A030310337, in part by the Science and Technology Program of Guangzhou City under Grant 201904010124, in part by the Guangdong Province Universities and Colleges Pearl River Scholar Funded Scheme under Grant 2017-ZJ022, in part by the Research Project of the Education Department of Guangdong Province under Grant 2017KTSCX060 and Grant 2017KZDXM028, in part by the Graduate Education and Innovation Project of Guangdong Province under Grant 2020SQXX12, and in part by the Guangdong Innovative Research Team Program under Grant 2014ZT05G157.

ABSTRACT As a class of convolutional error-correction codes (ECCs), spatially coupled protograph low-density parity-check (SC-PLDPC) codes with a sufficiently large coupling length can approach the channel capacity under belief propagation (BP) decoding. However, such codes suffer from poor performance in the case of small coupling lengths. To address the above weakness, we investigate the optimization and analysis of SC-PLDPC-coded bit-interleaved coded modulation (BICM) systems over Rayleigh fading channels. Specially, inspired by the unequal-error-protection (UEP) mechanism of M-ary phase-shift keying/quadrature amplitude modulation (M-PSK/QAM), we put forward a novel interleaver design scheme, referred to as *spatial position match mapping (SPMM) scheme*. Based on the mutual information (MI) analysis, the proposed interleaver can be used to significantly boost the performance of the SC-PLDPC codes in BICM systems. Furthermore, we propose a block-scheduling protograph-based extrinsic information transfer (BS-PEXIT) algorithm to estimate the convergence performance (i.e, decoding threshold) of the SPMM-aided SC-PLDPC codes in BICM scenarios. Simulation results are well consistent with the theoretical analyses, and show that the proposed SPMM-aided SC-PLDPC-coded BICM systems are superior to the state-of-the-art counterparts.

INDEX TERMS Spatially coupled protograph low-density parity-check (SC-PLDPC) codes, bit-interleaved coded modulation (BICM), interleaver, wireless fading channels.

I. INTRODUCTION

Bit-interleaved coded modulation (BICM) is of particular effectiveness to achieve both capacity-approaching performance and high transmission rate in various communication scenarios, e.g., wireless communications [1]–[4], vehicular communications [5], and aeronautical communications [6]–[8]. As one of the most critical techniques in BICM systems, error-correction codes (ECCs) must be carefully designed and optimized in order to enhance the reliability and quality of data transmission. In particular, protograph low-density parity-check (PLDPC) codes have attracted a great deal of attention in BICM scenarios owing to their excellent error performance and relatively low complexity. Moreover, much effort has been given to the advancement of theoretical-analysis tools, e.g., protograph-based extrinsic information transfer (PEXIT) algorithm [9], for PLDPC codes so as to predict the asymptotic performance of such codes and determine the best candidates for a specific communication scenario.

In PLDPC-coded BICM systems, the interleaver design can be considered as another important technique to enable additional performance gains by exploiting the unequal-error-protection (UEP) characteristic of high-order

The associate editor coordinating the review of this manuscript and approving it for publication was Jiankang Zhang.

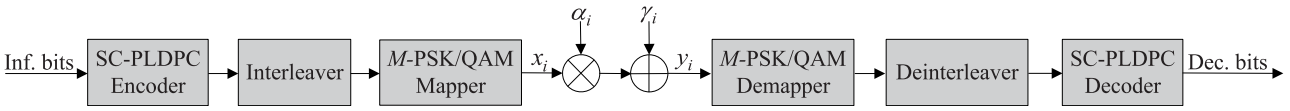

FIGURE 1. Block diagram of an SC-PLDPC-coded BICM system over Rayleigh fading channels.

modulations. For instance, an interleaving scheme, called *variable-degree matched mapping (VDMM)*, has been proposed for Gray-mapped BICM systems over additive white Gaussian noise (AWGN) channels [10] and Rayleigh fading channels [11]. Furthermore, an exhaustive-search-based method has been incorporated into VDMM so as to find the best permutation between the variable nodes (VNs) and the labeling bit positions [12]. In parallel with the above works, a variety of VN-degree-distribution-based and weight-distribution-based interleaving schemes have been developed in order to further enhance the performance of BICM systems [13], [14].

Motivated by the superiorities of PLDPC codes, a class of convolutional-like PLDPC codes, called *spatially coupled PLDPC (SC-PLDPC) codes*, has been widely investigated. Such codes not only benefit from relatively low complexity, but also approach the maximum-a-posteriori (MAP) thresholds under believe propagation (BP) decoding [15]–[17]. Thereby, the SC-PLDPC codes may have great potential to be incorporated into BICM systems [18]. In the case of a sufficiently large coupling length, the SC-PLDPC codes can achieve MAP-approaching performance due to the decoding-wave (i.e., threshold saturation) phenomenon [19]. Unfortunately, such codes have a large codeword length, which cannot satisfy the low-latency requirement of modern wireless communication systems. Besides, the SC-PLDPC codes suffer from relatively weaker decoding thresholds when the coupling length is small or moderate [20]. To deal with the above issue, some research effort has been devoted to the design and analysis of small-coupling-length SC-PLDPC codes [21]–[23] and small-constraint-length SC-PLDPC codes [24], [25] in order to achieve satisfactory decoding performance. In addition, the investigation regarding the performance improvement of finite-coupling-length SC-PLDPC codes in BICM scenarios has been conducted [26]. To be specific, an optimized bit-to-symbol mapping scheme, which combines bit allocation and shortened pattern, has been proposed for finite-coupling-length SC-PLDPC codes so as to improve their performance. Nevertheless, to the best of our knowledge, few works have been reported to investigate the interleaver design for SC-PLDPC-coded BICM systems under fading environments from the perspective of mutual information (MI) analysis.

In this paper, we study the design and analysis of SC-PLDPC-coded BICM systems over ergodic Rayleigh fading channels.[1] To be specific, we first propose a novel interleaver design scheme for SC-PLDPC-coded BICM systems, called as *spatial position match mapping (SPMM) scheme*, which guarantees that the VNs with different iterative convergence performance are properly mapped to the labeling bit positions with different bit-plane MIs. The proposed SPMM scheme can enhance the decoding-wave phenomenon in the joint demapping-and-decoding process, and thus significantly accelerate the convergence speed of the a-posteriori MIs for the SC-PLDPC codes in BICM systems. For further investigation, we propose a block-scheduling PEXIT (BS-PEXIT) algorithm to predict the convergence performance (i.e., decoding threshold) of the SPMM-aided SC-PLDPC codes in BICM scenarios. Theoretical analyses and simulation results show that our proposed SPMM-adied SC-PLDPC-coded BICM systems achieve better performance than the conventional counterparts.

The remainder of this paper is organized as follows. To begin with, the SC-PLDPC-coded BICM system model over Rayleigh fading channels is introduced in Section II. Then, the SPMM interleaving scheme is put forward in Section III. Section IV gives the BS-PEXIT algorithm for the SC-PLDPC-coded BICM systems. Simulation results are presented in Section V and conclusions are drawn in Section VI.

II. SYSTEM MODEL

A. SC-PLDPC-CODED BICM SYSTEMS

In this paper, we consider a BICM system with the use of SC-PLDPC codes, whose diagram is depicted in Fig. 1. First, the information bits (Inf. bits) are encoded to a coded bit sequence of length n by an SC-PLDPC encoder. Then, such a coded bit sequence is fed to an M-ary modulator after a specific permutation by an interleaver. Moreover, every $m = \log_2 M$ coded bits are mapped to a complex modulated symbol under a given constellation set χ, whose output is expressed as x_i $(i = 1, 2, ...n/m)$. These modulated symbols will be passed through an uncorrelated flat Rayleigh fading channel and their corresponding received signals can be written as

$$y_i = \alpha_i x_i + \gamma_i, \tag{1}$$

where α_i is the complex Gaussian-distributed fading factor; γ_i is a complex Gaussian noise with zero mean and variance $\sigma^2 = N_0/2$ in per dimension.

At the receiver, the received signals are processed by a soft-input soft-output (SISO) demapper and SC-PLDPC decoder. More specifically, the demapper and decoder are implemented via the max-sum approximation of the log-domain maximum a-posteriori probability (Max-log-Map) algorithm and the belief propagation (BP) algorithm [20], respectively.

[1] Although a Rayleigh fading channel is considered in this paper, the proposed design methods regarding the SPMM scheme and the BS-PEXIT algorithm can be also applicable to other types of ergodic channels, such as the AWGN channel.

B. SC-PLDPC CODES

A protograph can be regarded as a small Tanner graph [27] $\mathcal{G} = (\mathcal{V}, \mathcal{C}, \mathcal{E})$ consisting of three different sets, i.e., a VN set $\mathcal{V}$, a check node (CN) set $\mathcal{C}$, and an edge set $\mathcal{E}$. The cardinalities of $\mathcal{V}$, $\mathcal{C}$, and $\mathcal{E}$ correspond to N_v, N_c, and E, respectively. In a protograph, each edge $e_{i,j} \in \mathcal{E}$ connects a VN $v_j \in \mathcal{V}$ to a CN $c_i \in \mathcal{C}$, and parallel edges are permitted. Furthermore, a protograph with a code rate $R = (N_v - N_c)/N_t$ can be defined by a base matrix $\mathbf{B} = (b_{i,j})$ of size $N_c \times N_v$, where $b_{i,j}$ represents the number of edges connecting c_i to v_j, and N_t is the number of transmitted VNs. It should be noted that there is no punctured VNs in the case of $N_t = N_v$. An expanded protograph, namely derived graph, can be generated by performing a lifting operation for its corresponding protograph, and thus a protograph code with arbitrary length can be easily obtained.[2]

Based on a given protograph, its corresponding SC protograph can be built by applying a specific edge-spreading rule. Specifically, the formulation starts from replicating the protograph L times, and associating each duplicate with a time index t ($t = 0, 1, \ldots, L-1$). Then, one can connect the edges emanating from the VNs of protograph at times t ($t = 0, 1, \ldots, L-1$) over the CNs of protograph at times t' ($t' = t, t+1, \ldots, t+m_c$), where m_c denotes the constraint length ($0 < m_c < L$). From the perspective of matrix structure, the base matrix $\mathbf{B}$ corresponding to a protograph of size $N_c \times N_v$ can be decomposed into $m_c + 1$ submatrices, i.e, $\mathbf{B}_0, \mathbf{B}_1, \ldots, \mathbf{B}_{m_c}$. Their relationship satisfies the condition of $\mathbf{B} = \sum_{s=0}^{m_c} \mathbf{B}_s$. Based on the above discussion, in the case of no puncturing, the basic matrix of size $n_c \times n_v = N_c(L + m_c) \times N_v L$ corresponding to an SC-PLDPC code can be expressed as

$$\mathbf{B}^{\mathrm{SC-PLDPC}}_{[0,L-1]} = \overbrace{\begin{bmatrix} \mathbf{B}_0 & & & & \\ \mathbf{B}_1 & \mathbf{B}_0 & & & \\ \vdots & \mathbf{B}_1 & \ddots & & \\ \mathbf{B}_{m_c} & \vdots & \ddots & \mathbf{B}_0 & \\ & \mathbf{B}_{m_c} & & \mathbf{B}_1 & \\ & & \ddots & \vdots & \ddots \\ & & & \mathbf{B}_{m_c} & \ddots \end{bmatrix}}^{L} \begin{matrix} \\ \\ \\ \\ \\ \\ \end{matrix} \begin{matrix} \\ \\ \\ \mathbf{B}_0 \\ \mathbf{B}_1 \\ \ddots \\ \mathbf{B}_{m_c} \end{matrix} . \quad (2)$$

Case 1: For a sequence of L disjoint (d_v, d_c) regular protographs, one can formulate a (d_v, d_c, L) coupled chain by a specific SC operation, where d_v and d_c are the VN degrees and CN degrees, respectively. For instance, Fig. 2(a) shows the formulation process of $(3, 6, L)$ coupled chain corresponding to a (3, 6) SC-PLDPC code with coupling length L, where the black circles and white squares represent the VNs and CNs, respectively. In particular, the base matrix $\mathbf{B}^{(3,6)}$ and corresponding submatrices $\mathbf{B}_s^{(3,6)}(s = 0, 1, 2)$ for the (3, 6) protograph are denoted by

$$\mathbf{B}^{(3,6)} = [3\ 3], \quad \mathbf{B}_0^{(3,6)} = \mathbf{B}_1^{(3,6)} = \mathbf{B}_2^{(3,6)} = [1\ 1]. \quad (3)$$

Case 2: Similarly, the SC-PLDPC codes can be also constructed from irregular protographs. Referring to Fig. 2(b), a repeat-jagged-accumulate (RJA) SC-PLDPC code is constructed by its corresponding RJA protograph [29], whose base matrix $\mathbf{B}^{\mathrm{RJA}}$ and submatrices $\mathbf{B}_s^{\mathrm{RJA}}(s = 0, 1)$ are given as

$$\mathbf{B}^{\mathrm{RJA}} = \begin{bmatrix} 2 & 2 & 1 & 1 \\ 1 & 1 & 3 & 1 \end{bmatrix},$$
$$\mathbf{B}_0^{\mathrm{RJA}} = \begin{bmatrix} 1 & 1 & 1 & 0 \\ 0 & 1 & 2 & 1 \end{bmatrix}, \quad \mathbf{B}_1^{\mathrm{RJA}} = \begin{bmatrix} 1 & 1 & 0 & 1 \\ 1 & 0 & 1 & 0 \end{bmatrix}. \quad (4)$$

For a given coupling length L, the code rate R_L of an SC-PLDPC code can be given by

$$R_L = 1 - \frac{n_c}{n_v} = 1 - \frac{(L + m_c)N_c}{LN_v} = 1 - \left(\frac{L + m_c}{L}\right)(1 - R), \quad (5)$$

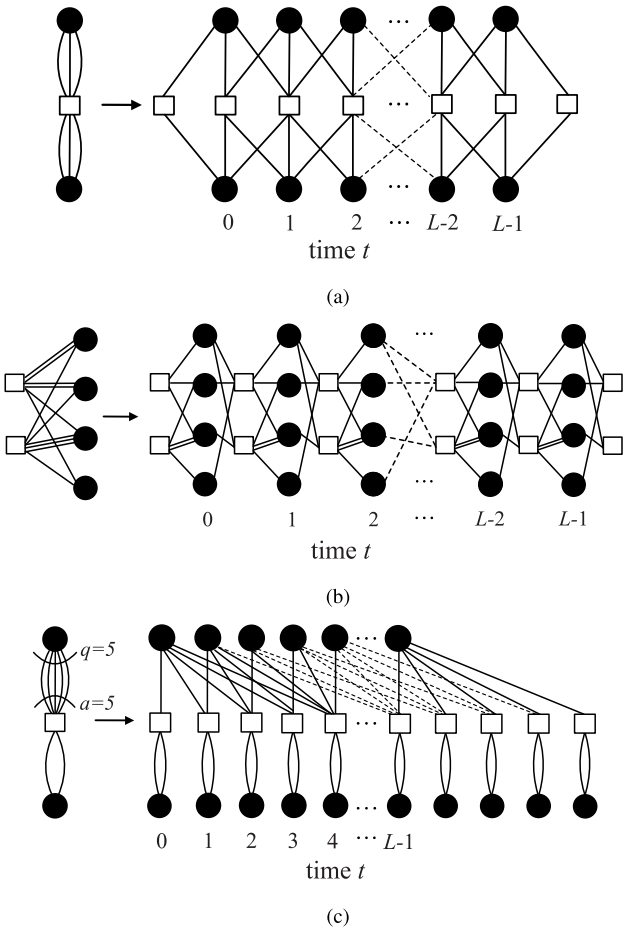

FIGURE 2. Protograph structures: (a) (3, 6) SC-PLDPC codes, (b) RJA SC-PLDPC codes, and (c) (5, 5) RA SC-PLDPC codes.

[2] Actually, the lifting procedure can be implemented by exploiting a modified progress-edge-growth (PEG) algorithm [28].

where n_c and n_v are the numbers of CNs and VNs in the corresponding base matrix, respectively; $R = 1 - N_c/N_v$ is the code rate of the original protograph code.

Case 3: Different from the above two cases, the formulation process of (q, a) RA SC-PLDPC codes can be considered as a special case, because additional $q - 1$ degree-2 VNs are needed to be added, where $q = a$ and they denote the degree of message-bit-related VNs and the number of edges between the CNs and the message-bit-related VNs [30], [31]. In order to make the formulation process more clear, Fig. 2(c) shows a specific example, i.e., a (5, 5) RA SC-PLDPC code. For a given coupling length L, the code rate of a (q, a) RA SC-PLDPC code can be calculated as

$$R_L^{\mathrm{RA}} = 1 - \frac{L + (q-1)}{N_v L + q - 1}. \tag{6}$$

III. INTERLEAVER DESIGN FOR SC-PLDPC-CODED BICM SYSTEMS

A. PROPOSED SPMM SCHEME

As the coupling length L tends to infinity, the SC-PLDPC codes can attain desirable threshold improvements. But a large L leads to a large codeword length, which makes the SC-PLDPC codes rather difficult to meet the low-complexity requirement in wireless communication scenarios [30], [32]. To address this weakness, some research works related to the performance analysis and structure optimization of finite-coupling-length SC-PLDPC codes have been investigated. For instance, a scaling law has been proposed to predict the finite-coupling-length performance of the SC-PLDPC codes [33]. Moreover, additional encoding structures have been considered incorporating into the boundaries of the finite-coupling-length SC-PLDPC codes so as to enhance their error performance [21], [34]. In addition to the above code-design schemes, the performance of the finite-coupling-length SC-PLDPC codes can also be improved from the perspective of MI convergence. It is well known that the MIs corresponding to the coded bits at both ends of the codeword are capable of realizing fast convergence, while the remaining coded bits suffer from poor convergence performance, which severely degrades the decoding thresholds of the SC-PLDPC codes. With an aim to improve the threshold performance, we propose a novel interleaving scheme, called *SPMM scheme*, to protect some coded bits based on the UEP property of the bit-to-symbol-mapping process in BICM systems. The proposed SPMM scheme not only can maintain the same implementation complexity as the original systems, but also can enhance the decoding-wave effect so as to accelerate the convergence performance of the SC-PLDPC codes. In the following, we will briefly describe the principle of the proposed SPMM scheme, which can be considered as a two-step design method.

1) MI-BASED BLOCK SCHEDULING

In an M-ary BICM system with the sequential mapping scheme [35], [36], the a-posteriori MIs of all VNs in a given SC protograph can be calculated based on the conventional PEXIT algorithm, and the convergence tendency of each VN can be predicted by analyzing its corresponding MI value, i.e., the larger the MI value of a VN is, the better the convergence performance of the VN can be realized. Then, according to the relationship between the SC-PLDPC code and its corresponding SC protograph, i.e., i) an SC-PLDPC code of length $n = n_v \times p$ can be obtained by implementing p times lifting operation on its corresponding SC protograph of length n_v; ii) the entire SC-PLDPC codeword can be divided into n_v blocks in a sequential order, and each block consisting of p coded bits corresponds to a VN of the SC protograph; the convergence tendency of each block in the SC-PLDPC code can be evaluated. Afterwards, by comparing the MI convergence differences among the n_v blocks, one can use a "high-to-low MI-based scheduling" rule to adjust the original block sequence $\{V_{B,1}, V_{B,2}, \ldots, V_{B,n_v}\}$ in a descending order, i.e., the block with the largest MI is placed at the first position, while the other blocks with relatively low MIs are followed. Based on the above operation, one can obtain an optimized block sequence $\{V'_{B,1}, V'_{B,2}, \ldots, V'_{B,n_v}\}$, and it will be further processed in the next step.

2) UEP-BASED GROUP MAPPING

For a given M-ary constellation, there exist M different labels and each of which is formulated by $m = \log_2 M$ labeling bit positions $x^{b_1}, x^{b_2}, \ldots, x^{b_m}$.[3] Inspired by the protection-level difference among the labeling bit positions (i.e., UEP characteristic), some specific coded bits within the optimized block sequence $\{V'_{B,1}, V'_{B,2}, \ldots, V'_{B,n_v}\}$ can be protected with relatively higher priorities so as to improve the convergence performance of the entire SC-PLDPC codeword. To be specific, the above optimized block sequence can be equally divided into m groups $V_{G,1}, V_{G,2}, \ldots, V_{G,m}$ in a sequential order, which ensure that the convergence performance of these m groups can satisfy the condition $I_{G,1} \geq I_{G,2} \geq \cdots \geq I_{G,m}$, where $I_{G,k} (k = 1, 2, \ldots, m)$ denotes the average MI (AMI) of the k-th group. Afterwards, during the bit-to-symbol mapping process, every m coded bits, which are separately extracted from the m different groups, can be respectively assigned into the m labeling bit positions with different protection levels based on a "reverse water-filling" rule. In particular, the coded bits, which are extracted from the groups with relatively good convergence performance, are assigned into the labeling bit positions with relatively low protection level. According to the above operation, one can guarantee that the coded bits with poor convergence performance in the SC-PLDPC codeword can be protected with relatively higher priorities and the wave-like convergence can be further enhanced.

In general, the principle of the proposed SPMM scheme for the SC-PLDPC-coded BICM systems is illustrated in Fig. 3.

[3] In particular, these m labeling bit positions (i.e., $x^{b_1}, x^{b_2}, \ldots, x^{b_m}$) possess different protection levels, which can be evaluated by the bit-plane MI $I(x^{b_k}; y)$ between the labeling bit position x^{b_k} and the received signal y, where $k = 1, 2, \ldots, m$ [10]. Moreover, for an M-ary constellation, the l-th label $x_l \triangleq \left\{x_l^{b_1}, x_l^{b_2}, \ldots, x_l^{b_m}\right\}$.

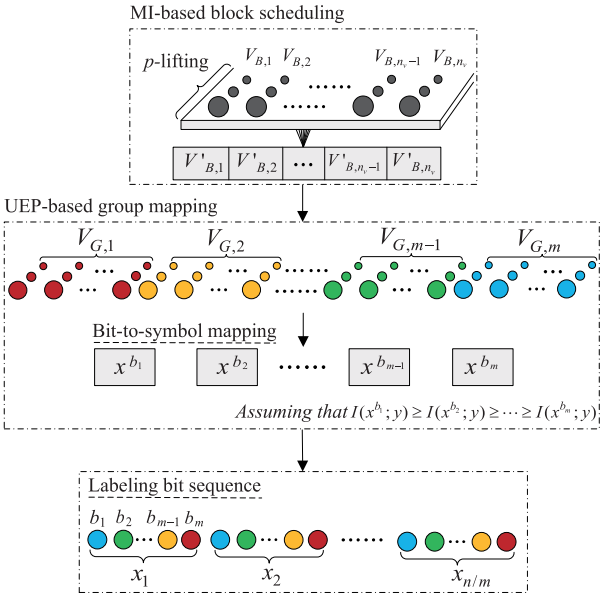

FIGURE 3. The principle of the SPMM scheme for an SC-PLDPC-coded BICM system with an *M*-ary constellation.

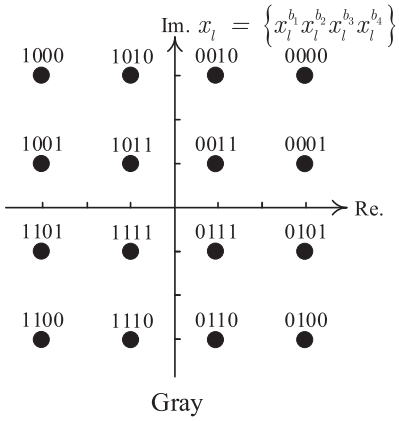

FIGURE 4. Gray constellation for the 16-QAM modulation.

One can easily find that the proposed SPMM scheme can substantially exploit the convergence feature of SC-PLDPC codes and the UEP characteristic of labeling bit positions so as to balance the convergence speed and enhance the wave-like convergence. To further clearly elaborate on the proposed SPMM scheme, three specific examples are shown as follows.

Example: For the BICM system with the Gray-mapped 16-QAM modulation (see Fig. 4) and the (3, 6) SC protograph of length $n_v = 24$, the convergence performance of all the 24 VNs can be predicted based on the conventional PEXIT algorithm, and the detailed MI convergence tendency can be observed from Fig. 5(a). Then, by implementing the p-times lifting operation on such an SC protograph, a (3, 6) SC-PLDPC code of length $n = 24 \times p$ can be obtained, and the convergence tendency of the original block sequence $\{V_{B,1}, V_{B,2}, \ldots, V_{B,24}\}$ can also be evaluated. Following the

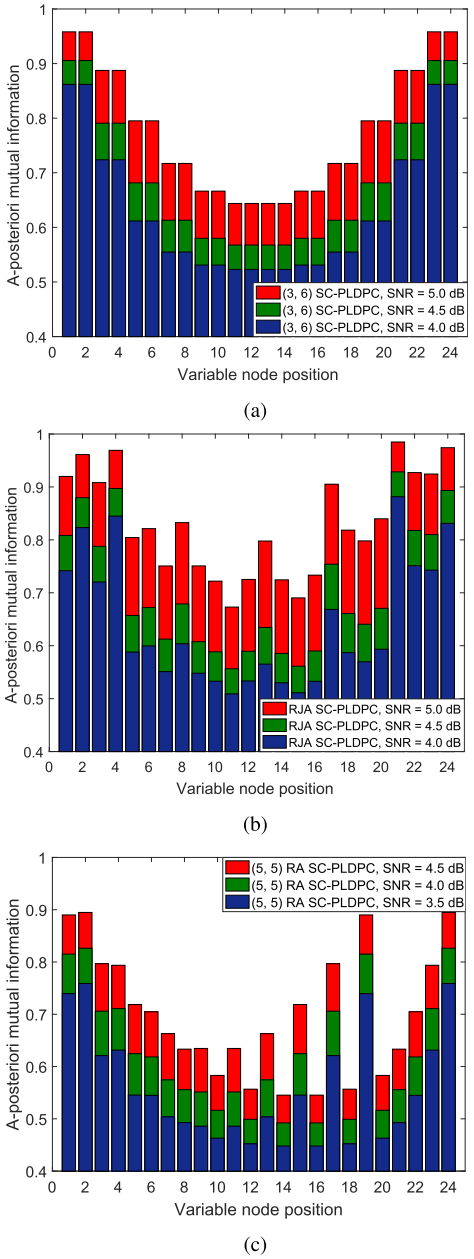

FIGURE 5. The a-posteriori MIs of (a) (3, 6) SC-PLDPC code, (b) RJA SC-PLDPC code, and (c) (5, 5) RA SC-PLDPC code at different SNR values. A Gray-mapped 16-QAM BICM system over Rayleigh fading channels is considered.

high-to-low MI-based scheduling rule of Step 1, the corresponding optimized block sequence $\{V'_{B,1}, V'_{B,2}, \ldots, V'_{B,24}\}$ can be obtained, and which is divided into $m = 4$ groups $V_{G,1}, V_{G,2}, V_{G,3}, V_{G,4}$ in a sequential order. According to the reverse water-filling rule of Step 2 and the property of these bit-plane MIs in the Gray-mapped 16-QAM constellation, i.e.,

$$I(x^{b_1}; y) = I(x^{b_2}; y) > I(x^{b_3}; y) = I(x^{b_4}; y),$$

the coded bits, which are extracted from the 4 different groups (i.e., $V_{G,1}, V_{G,2}, V_{G,3}, V_{G,4}$), can be assigned into 4 different

labeling bit positions (i.e., $x^{b_4}, x^{b_3}, x^{b_2}, x^{b_1}$), respectively. Based on the above SPMM scheme, the wave-like convergence of the $(3, 6)$ SC-PLDPC code can be effectively enhanced, and its convergence performance can be further improved.

Likewise, for the Gray-mapped 16-QAM BICM system and the RJA SC protograph of length $n_v = 24$, the convergence performance of all the 24 VNs can be predicted, and which can be found in Fig. 5(b). Exploiting the convergence feature of the RJA SC-PLDPC code generated from the above protograph and the UEP characteristic of labeling bit positions, one can also implement the proposed SPMM scheme on the RJA SC-PLDPC code so as to enhance its wave-like convergence.

To further explore the feasibility of the proposed SPMM scheme, the $(5, 5)$ RA SC-PLDPC code generated from the $(5, 5)$ RA SC protograph of length $n_v = 24$ is also considered. Referring to Fig. 5(c), the convergence tendency of all the 24 VNs in its protograph is shown. Based on the MI convergence difference, the proposed SPMM scheme can also be implemented for the $(5, 5)$ RA SC-PLDPC code in order to improve its threshold performance.

Note also that:

- Although we only assume 16-QAM modulation in the three specific examples, the proposed SPMM scheme is also feasible to other high-order modulations, such as the 8-PSK and 64-QAM modulations (see Sect. IV-B).
- To make the above three specific examples more compact and clear, we adopt an unified length n_v for three different types of SC protographs. Nonetheless, the proposed SPMM scheme is also applicable to other SC protographs and different lengths n_v (see Sect. IV-B).
- In the conventional VDMM scheme [10], the permutation pattern between the VNs and the labeling bit positions follows a fixed order, i.e., the VNs with higher degree are assigned into the labeling bit positions with higher protection level, and thus the VDMM scheme is tailored for the conventional irregular protograph codes and no longer effective for SC protograph codes. The convergence principle of the proposed SPMM scheme is quite different from that of the existing techniques. In our proposed SPMM scheme, the UEP characteristic of the bit-to-symbol-mapping process is exploited to balance the convergence speed of all the VNs as much as possible. For this reason, the proposed SPMM scheme is available for both regular and irregular protograph-based codes, especially for the SC protograph codes.
- In general, the SC-PLDPC codes with a small coupling length L suffer from a rate loss and undesirable decoding threshold, while the SC-PLDPC codes with a large coupling length suffer from high decoding complexity and latency. Using puncturing schemes [21] or incorporating some additional encoding structures (e.g., some VNs) into the boundaries of an SC-PLDPC code [34] can effectively alleviate the rate-loss issue.

IV. BS-PEXIT ALGORITHM AND PERFORMANCE ANALYSIS FOR SC-PLDPC-CODED BICM SYSTEMS

A. BS-PEXIT ALGORITHM

With an aim to accurately predict the convergence performance of SC-PLDPC codes in the SPMM-aided BICM systems, a modified PEXIT algorithm, referred to as *BS-PEXIT algorithm*, has been proposed in this subsection. Specifically, the BS-PEXIT algorithm not only can be utilized to trace the MI convergence behavior in the iterative decoding process, but also can calculate the minimum signal-to-noise ratio (SNR) (i.e., decoding threshold) that allows the system realizing error-free transmission. To facilitate the illustration of such an algorithm, some concepts are defined as follows.

In an M-ary BICM system, the initial channel log-likelihood ratio (LLR) of the coded bit l_i^k, which corresponds to the k-th labeling bit position within the i-th symbol $x_i^{b_k}$, can be derived as Eq. 7, where $\chi^{b_k=0}$ and $\chi^{b_k=1}$ denote the subset of the constellation set χ with $b_k = 0$ and that with $b_k = 1$, respectively; $P_r(\cdot)$ is the probability density function.

$$l_i^k = \ln \frac{P_r(x_i^{b_k} = 0|y_i, \alpha_i)}{P_r(x_i^{b_k} = 1|y_i, \alpha_i)} = \ln \frac{\sum\limits_{x_i \in \chi^{b_k=0}} \exp\left\{-\frac{1}{2\sigma^2}(y_i - \alpha_i x_i)^2\right\}}{\sum\limits_{x_i \in \chi^{b_k=1}} \exp\left\{-\frac{1}{2\sigma^2}(y_i - \alpha_i x_i)^2\right\}}. \tag{7}$$

For the given LLR $l_i^k \sim \mathcal{N}(\sigma_{\text{ch}}^2/2, \sigma_{\text{ch}}^2)$, the MI between the coded bit and its associated l_i^k is represented by $J(\sigma_{\text{ch}})$ and given as

$$J(\sigma_{\text{ch}}) = 1 - \int_{-\infty}^{+\infty} \frac{\exp\left(-\frac{(\mu - \sigma_{\text{ch}}^2/2)^2}{2\sigma_{\text{ch}}^2}\right)}{\sqrt{2\pi\sigma_{\text{ch}}^2}} \times \log_2[1 + \exp(-\mu)]\, \mathrm{d}\mu. \tag{8}$$

The derivation of $J(\cdot)$ and its inverse function $J^{-1}(\cdot)$ can be obtained in [36]. In addition, several different types of MIs for the SC-PLDPC-coded BICM systems are briefly illustrated as follows.

- I_{ED} is denoted as the *extrinsic* MI of the demapper.
- $I_{\text{AV}}(i, j)$ and $I_{\text{AC}}(i, j)$ are denoted as the *a-prior* MI transmitted from c_i to v_j and v_j to c_i, respectively.
- $I_{\text{EV}}(i, j)$ and $I_{\text{EC}}(i, j)$ are denoted as the *extrinsic* MI transmitted from v_j to c_i and c_i to v_j, respectively.
- $I_{\text{APP}}(j)$ is denoted as the *a-posteriori* MI of v_j.

In particular, the maximum number of iterations in such an algorithm is set to $T_{\max}$. Moreover, there is an exchange of MI from VN to CN and vice versa in each iteration, i.e., $I_{\text{AV}}(i, j) = I_{\text{EC}}(i, j)$ and $I_{\text{AC}}(i, j) = I_{\text{EV}}(i, j)$. Based on the aforementioned definitions, the BS-PEXIT algorithm can be illustrated as below.

1) **Initialization:** At the beginning of the algorithm, there exists an initial E_b/N_0, which is served as an input parameter in the demapper.

2) **Updating the *extrinsic* MI of demapper:** Based on the SPMM-based Monte-Carlo simulation, the *extrinsic* LLRs corresponding to the coded bits output from the demapper can be obtained, and they will be scheduled by a specific deinterleaver so as to be an original sequential order corresponding to the SC-PLDPC codes before being interleaved. Then, the *extrinsic* MIs I_{ED}^{j} ($j = 1, 2, \ldots, n_v$), which are regarded as the initial decoding information of the VNs in the SC-PLDPC decoder, can be calculated by [11]

$$I_{\mathrm{ED}}^{j} = 1 - \mathbb{E}\left[\log_2(1 + e^{-\widetilde{u}_z l_z})\right], \tag{9}$$

where $\mathbb{E}[\cdot]$ denotes the expectation function; $\widetilde{u}_z \in \{+1, -1\}$ denotes the binary-phase shift-keying (BPSK) modulated symbol corresponding to the z-th coded bit; l_z denotes the *extrinsic* LLR of the z-th coded bit; and $z = (j-1) \times p + 1, (j-1) \times p + 2, \ldots, (j-1) \times p + p$. In particular, p is a lifting factor for the corresponding SC protograph. Furthermore, the *extrinsic* MIs are passed to the decoder and served as the initial channel MIs of the VN decoder, i.e., $I_{\mathrm{CH}}^{j} = I_{\mathrm{ED}}^{j}$ for $j = 1, 2, \ldots, n_v$.

3) **Calculating the *extrinsic* MI from VN to CN:** For $i = 1, 2, \ldots, n_c$ and $j = 1, 2, \ldots, n_v$, the *extrinsic* MI $I_{\mathrm{EV}}(i, j)$ transmitted from the VN v_j to the CN c_i can be calculated as

$$I_{\mathrm{EV}}(i,j) = J\left(\sqrt{\left(\sum_{s \neq i} b_{s,j}[J^{-1}(I_{\mathrm{AV}}(s,j))]^2 + (b_{i,j}-1)[J^{-1}(I_{\mathrm{AV}}(i,j))]^2 + [J^{-1}(I_{\mathrm{CH}}^{j})]^2\right)}\right). \tag{10}$$

4) **Calculating the *extrinsic* MI from CN to VN :** For $i = 1, 2, \ldots, n_c$ and $j = 1, 2, \ldots, n_v$, the *extrinsic* MI transmitted from the CN c_i to the VN v_j is measured by

$$I_{\mathrm{EC}}(i,j) = 1 - J\left(\sqrt{\left(\sum_{s \neq j} b_{i,s}[J^{-1}(1 - I_{\mathrm{AC}}(i,s))]^2 + (b_{i,j}-1)[J^{-1}(1 - I_{\mathrm{AC}}(i,j))]^2\right)}\right). \tag{11}$$

5) **Calculating the *a-posteriori* MI of VNs:** For $j = 1, 2, \ldots, n_v$, the *a-posteriori* MI of VN v_j can be calculated by exploiting $I_{\mathrm{AV}}(i, j)$ and I_{CH}^{j}, as

$$I_{\mathrm{APP}}(j) = J\left(\sqrt{\left(\sum_{i=1}^{n_v} b_{i,j}[J^{-1}(I_{\mathrm{AV}}(i,j))]^2 + [J^{-1}(I_{\mathrm{CH}}^{j})]^2\right)}\right). \tag{12}$$

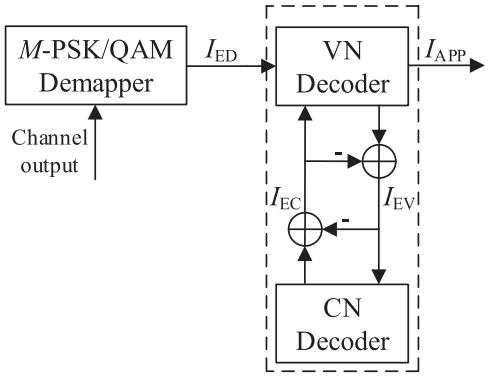

FIGURE 6. MI update process of an SC-PLDPC code in the BS-PEXIT algorithm over Rayleigh fading channels.

6) **Finalization:** The iterative process is terminated when the *a-posteriori* MI $I_{\mathrm{APP}}(j) = 1$ for $j = 1, 2, \ldots, n_v$, or when the maximum number of iterations is reached. Otherwise, we repeat Steps 3)-5) continuously.

Based on the BS-PEXIT algorithm, one can get the smallest E_b/N_0, referred to as *decoding threshold*, that guarantees the *a-posteriori* MIs of all VNs in an SC-PLDPC code converging to the value of unity. For further illustration, the MI update process of an SC-PLDPC code in the BS-PEXIT algorithm is described in Fig. 6.

Note also that:

- Due to the characteristic of the proposed SPMM scheme, i.e., the coded bits are interleaved based on the convergence performance analysis, a specific deinterleaving operation must be considered before calculating the *extrinsic* MI I_{ED}.
- In the conventional PEXIT analysis, only one *extrinsic* MI I_{ED} can be obtained. However, in the proposed BS-PEXIT analysis, there exist n_v *extrinsic* MI I_{ED}^{j} ($j = 1, 2, \ldots, n_v$) output from the demapper, because the proposed SPMM scheme is incorporated into the Monte-Carlo simulation.

B. DECODING THRESHOLD ANALYSIS

Based on the proposed BS-PEXIT algorithm, we estimate the decoding thresholds of three different types of SC-PLDPC codes, i.e., (i) (3, 6) SC-PLDPC code [20], (ii) RJA SC-PLDPC code [29], and (iii) (5, 5) RA SC-PLDPC code [37], with different coupling lengths in the Gray-mapped 16-QAM BICM systems. As observed from Tabel 1, considering the (3, 6) SC-PLDPC code, we adopt three different code rates, i.e., $R_L^{(3,6)} = 3/8, 2/5, 5/12$, which can be realized by setting the coupling length $L = 8, 10, 12$, respectively. Obviously, with the help of the proposed SPMM interleaving scheme, the (3, 6) SC-PLDPC code can exhibit smaller decoding thresholds in the case of three different coupling lengths (i.e., $L = 8, 10, 12$). This implies that the proposed SPMM interleaving scheme can effectively improve the threshold performance of the (3, 6) SC-PLDPC code with

TABLE 1. Decoding thresholds $(E_b/N_0)_{\text{th}}$ (dB) of the (3, 6) SC-PLDPC code, RJA SC-PLDPC code, and (5, 5) RA SC-PLDPC code with different coupling lengths in the Gray-mapped 16-QAM BICM system over Rayleigh fading channels.

Rate	(3, 6) SC-PLDPC [20]			RJA SC-PLDPC [29]			(5, 5) RA SC-PLDPC [37]		
	L	Conventional	SPMM-aided	L	Conventional	SPMM-aided	L	Conventional	SPMM-aided
3/8	8	4.956	4.506	4	4.741	4.297	6	4.293	4.011
2/5	10	5.058	4.748	5	4.891	4.438	8	4.586	4.224
5/12	12	5.109	4.921	6	5.058	4.608	10	4.761	4.531

TABLE 2. Decoding thresholds $(E_b/N_0)_{\text{th}}$ (dB) of the (3, 6) SC-PLDPC code with different coupling lengths in the Gray-mapped 8-PSK and 64-QAM BICM systems.

Modulation	(3, 6) SC-PLDPC [20]			
	Rate	L	Conventional	SPMM-aided
8-PSK	7/18	9	4.324	3.835
	5/12	12	4.327	3.913
64-QAM	7/18	9	7.519	6.965
	5/12	12	7.613	7.463

small coupling length. Similar conclusions can be drawn from the RJA SC-PLDPC code and the (5, 5) RA SC-PLDPC code.

To get further insight, we compare the decoding thresholds of (i) (3, 6) SC-PLDPC code and (ii) SPMM-aided (3, 6) SC-PLDPC code in the Gray-mapped 8-PSK/64-QAM BICM systems.[4] As seen from Tabel 2, the SPMM-aided (3, 6) SC-PLDPC code can exhibit smaller decoding thresholds than its original (3, 6) SC-PLDPC code. This suggests that the proposed SPMM interleaving scheme is also preferable for the SC-PLDPC codes in other high-order modulated systems (e.g., 8-PSK and 64-QAM modulated systems).

Remark: Because the Gray constellation is considered as an optimal mapping scheme in the BICM systems [1], we mainly take it into account in this paper. Although we only consider three different types of SC-PLDPC codes for simulations, but the proposed SPMM interleaving scheme and BS-PEXIT algorithm are also applicable to other constellation mappers and other SC-PLDPC codes.

V. SIMULATION RESULTS

In this section, we provide some simulation results for three different types of SC-PLDPC codes, i.e., (i) (3, 6) SC-PLDPC code [20], (ii) RJA SC-PLDPC code [29], and (iii) (5, 5) RA SC-PLDPC code [37], with different coupling lengths in the Gray-mapped 8-PSK/16-QAM/64-QAM BICM systems over Rayleigh fading channels. In particular, we assume that the transmitted codeword length of all the above mentioned SC-PLDPC codes is set as $n = 4800$. Moreover, the maximum numbers of BP iterations is set as $T_{\text{BP}} = 100$.

A. BER PERFORMANCE FOR THE 16-QAM BICM SYSTEMS

For the Gray-mapped 16-QAM BICM systems, we study the simulated bit error rate (BER) of the regular SC-PLDPC code, i.e., (3, 6) SC-PLDPC code, with different coupling lengths. As observed from Fig. 7, with the help of the proposed SPMM interleaving scheme, the (3, 6) SC-PLDPC code can achieve significant gains under the condition of $L = 8, 10, 12$. Specially, the SPMM-aided (3, 6) SC-PLDPC codes benefit from performance gains of about $0.2 \sim 0.4$ dB with respect to the conventional (3, 6) SC-PLDPC codes at a BER of 10^{-6}.

Likewise, the SPMM interleaving scheme can make the irregular SC-PLDPC code, i.e., RJA SC-PLDPC code, achieving excellent performance. Referring to Fig. 8, the SPMM-aided RJA SC-PLDPC codes with coupling lengths $L = 4, 5, 6$ can obtain performance gains of about $0.3 \sim 0.4$ dB compared with the corresponding counterparts.

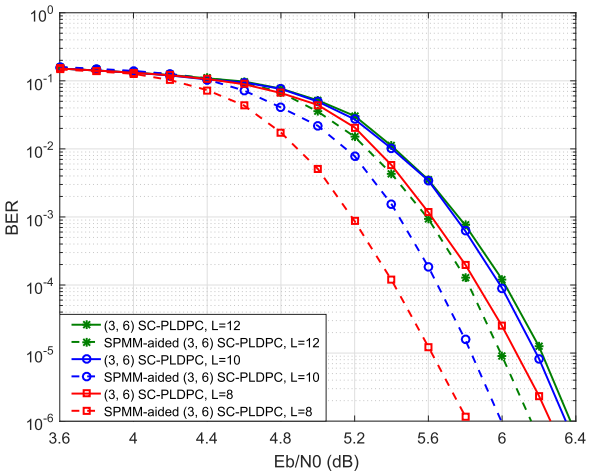

FIGURE 7. BER performance curves of the (3, 6) SC-PLDPC codes with coupling lengths $L = 8, 10, 12$ in the Gray-mapped 16-QAM BICM systems over a Rayleigh fading channel.

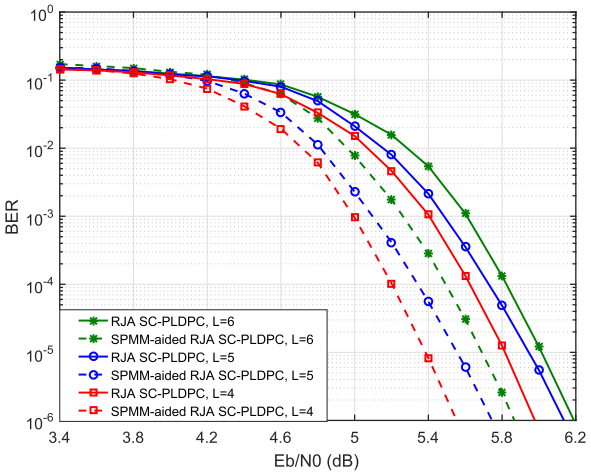

FIGURE 8. BER performance curves of the RJA SC-PLDPC codes with coupling lengths $L = 4, 5, 6$ in the Gray-mapped 16-QAM BICM systems over a Rayleigh fading channel.

[4]It should be noted that the Gray constellation cannot be formulated in the 32-QAM BICM systems [38], and thus we consider the Gray-mapped 8-PSK/64-QAM BICM systems in this paper so as to illustrate the effectiveness of the proposed SPMM interleaving scheme and BS-PEXIT algorithm.

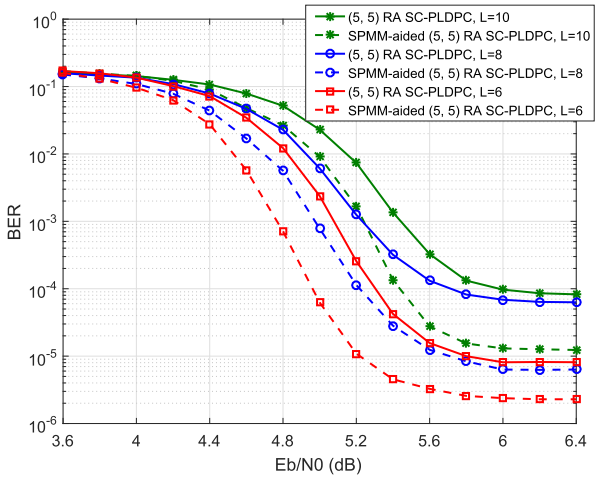

FIGURE 9. BER performance curves of the (5, 5) RA SC-PLDPC codes with coupling lengths $L = 6, 8, 10$ in the Gray-mapped 16-QAM BICM systems over a Rayleigh fading channel.

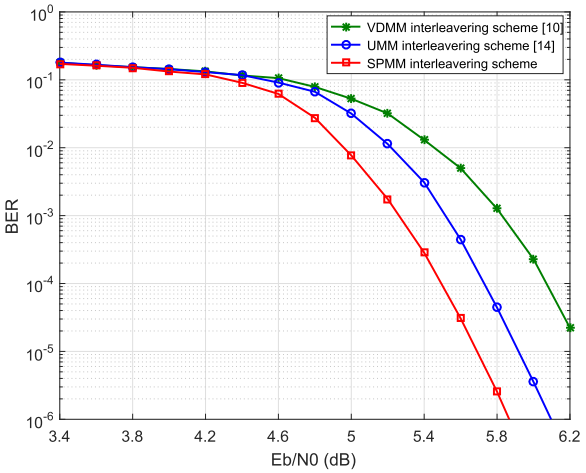

FIGURE 10. BER performance curves of the RJA SC-PLDPC code with coupling length $L = 6$ in the Gray-mapped 16-QAM BICM systems over a Rayleigh fading channel. Three different interleaving schemes are considered.

To further validate the proposed SPMM interleaving scheme, we perform simulations on the (5, 5) RA SC-PLDPC codes with coupling lengths $L = 6, 8, 10$. In Fig. 9, the proposed SPMM interleaving scheme not only can greatly enhance the BER performance of the (5, 5) RA SC-PLDPC codes, but also can further improve their error-floor phenomenon.[5] From the above discussions, the three different BER simulations verify the effectiveness of the proposed SPMM interleaving scheme, and which is consistent well with the proposed threshold analyses in Sect. IV.

B. BER COMPARISON AMONG DIFFERENT INTERLEAVING SCHEMES

To verify the superiorities of the proposed SPMM interleaving scheme, two different types of state-of-the-art counterparts, i.e., VDMM [10] and universal matched mapping (UMM) [14], are used as benchmarks for performance comparison. As seen from Fig. 10, the SPMM interleaving scheme can make the RJA SC-PLDPC code with coupling length $L = 6$ exhibiting the optimal performance in the Gray-mapped 16-QAM BICM systems. It is noteworthy that the above two counterparts, i.e., the VDMM and UMM interleaving schemes, are only applicable to the irregular protograph-based codes, and thus the RJA SC-PLDPC code is exploited as the baseline.

C. BER PERFORMANCE FOR THE BICM SYSTEMS WITH 8-PSK AND 64-QAM MODULATIONS

As a final example, we further perform simulations on the (3, 6) SC-PLDPC code with coupling length $L = 9$ in the Gray-mapped 8-PSK and 64-QAM BICM systems. As observed from Fig. 11, one can easily find that the

[5]It should be noted that the minimum distance of an RA code does not grow linearly with the codeword length, and thus the RA code, especially the RA SC-PLDPC code, suffers from error floor in the high-SNR region [37].

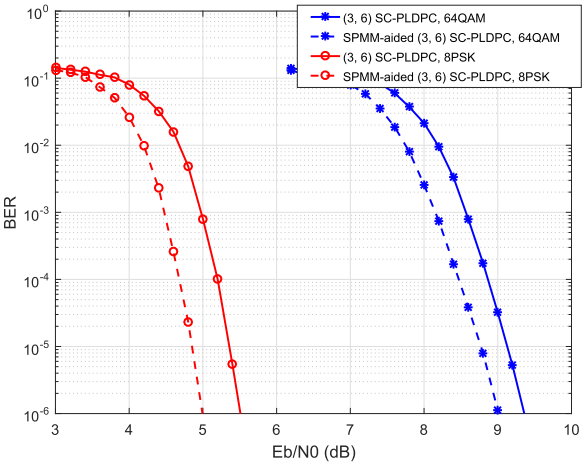

FIGURE 11. BER performance curves of the (3, 6) SC-PLDPC code with coupling length $L = 9$ in the Gray-mapped 8-PSK and 64-QAM BICM systems over a Rayleigh fading channel.

(3, 6) SC-PLDPC code with the proposed SPMM interleaving scheme can achieve better performance in contrast with the original counterpart, while the 8-PSK modulated system is considered. Moreover, similar conclusions can be drawn from the 64-QAM modulated system. This implies that the proposed SPMM interleaving scheme is feasible to the BICM systems with various modulated order.

VI. CONCLUSION

In this paper, we have conducted a comprehensive study on the finite-coupling-length SC-PLDPC-coded BICM systems over Rayleigh fading channels. Specially, we have conceived a novel interleaver design scheme, called *SPMM scheme*, which can be utilized to significantly improve the error performance of SC-PLDPC codes in BICM systems. In addition, we have developed a modified PEXIT algorithm, called *BS-PEXIT algorithm*, to predict the asymptotic convergence performance (i.e., decoding threshold) of the

SPMM-aided SC-PLDPC codes in the BICM systems. Theoretical analyses and simulation results have demonstrated that the SPMM-aided SC-PLDPC codes can achieve better performance than their original counterparts. Thanks to the above superiorities, the proposed SPMM-aided SC-PLDPC-coded BICM scheme stands out as a promising candidate for future wireless communication applications.

REFERENCES

[1] G. Caire, G. Taricco, and E. Biglieri, "Bit-interleaved coded modulation," *IEEE Trans. Inf. Theory*, vol. 44, no. 3, pp. 927–946, May 1998.

[2] J. Zhang, S. Chen, X. Guo, J. Shi, and L. Hanzo, "Boosting fronthaul capacity: Global optimization of power sharing for centralized radio access network," *IEEE Trans. Veh. Technol.*, vol. 68, no. 2, pp. 1916–1929, Feb. 2019.

[3] P. Chen, Z. Xie, Y. Fang, Z. Chen, S. Mumtaz, and J. J. P. C. Rodrigues, "Physical-layer network coding: An efficient technique for wireless communications," *IEEE Netw.*, to be published.

[4] Y. Fang, P. Chen, G. Cai, F. C. M. Lau, S. C. Liew, and G. Han, "Outage-limit-approaching channel coding for future wireless communications: Root-protograph low-density parity-check codes," *IEEE Veh. Technol. Mag.*, vol. 14, no. 2, pp. 85–93, Jun. 2019.

[5] J. Guo, B. Song, F. R. Yu, Y. Chi, and C. Yuen, "Fast video frame correlation analysis for vehicular networks by using CVS–CNN," *IEEE Trans. Veh. Technol.*, vol. 68, no. 7, pp. 6286–6292, Jul. 2019.

[6] J. Zhang, S. Chen, R. G. Maunder, R. Zhang, and L. Hanzo, "Regularized zero-forcing precoding-aided adaptive coding and modulation for large-scale antenna array-based air-to-air communications," *IEEE J. Sel. Areas Commun.*, vol. 36, no. 9, pp. 2087–2103, Sep. 2018.

[7] J. Zhang, T. Chen, S. Zhong, J. Wang, W. Zhang, X. Zuo, R. G. Maunder, and L. Hanzo, "Aeronautical *Ad Hoc* networking for the Internet-above-the-clouds," *Proc. IEEE*, vol. 107, no. 5, pp. 868–911, May 2019.

[8] J. Zhang, S. Chen, R. G. Maunder, R. Zhang, and L. Hanzo, "Adaptive coding and modulation for large-scale antenna array-based aeronautical communications in the presence of co-channel interference," *IEEE Trans. Wireless Commun.*, vol. 17, no. 2, pp. 1343–1357, Feb. 2018.

[9] G. Liva and M. Chiani, "Protograph LDPC codes design based on EXIT analysis," in *Proc. IEEE Global Telecommun. Conf.*, Nov. 2007, pp. 3250–3254.

[10] D. Divsalar and C. Jones, "Protograph based low error floor LDPC coded modulation," in *Proc. IEEE Military Commun. Conf.*, Mar. 2006, pp. 378–385.

[11] T. Van Nguyen, A. Nosratinia, and D. Divsalar, "Threshold of protograph-based LDPC coded BICM for Rayleigh fading," in *Proc. IEEE Global Telecommun. Conf.*, Dec. 2011, pp. 1–5.

[12] Y. Jin, M. Jiang, and C. Zhao, "Optimized variable degree matched mapping for protograph LDPC coded modulation with 16QAM," in *Proc. 6th Int. Symp. Turbo Codes Iterative Inf. Process.*, Sep. 2010, pp. 161–165.

[13] A. Alvarado, E. Agrell, L. Szczecinski, and A. Svensson, "Unequal error protection in BICM with QAM constellations: Interleaver and code design," in *Proc. IEEE Int. Conf. Commun.*, Jun. 2009, pp. 1–6.

[14] X. Liu, Y. Wei, and M. Jiang, "A universal interleaver design for bit-interleaved QC-LDPC coded modulation," in *Proc. 9th Int. Conf. Wireless Commun. Signal Process. (WCSP)*, Oct. 2017, pp. 1–6.

[15] M. Lentmaier, A. Sridharan, D. J. Costello, and K. S. Zigangirov, "Iterative decoding threshold analysis for LDPC convolutional codes," *IEEE Trans. Inf. Theory*, vol. 56, no. 10, pp. 5274–5289, Oct. 2010.

[16] S. Kudekar, T. Richardson, and R. L. Urbanke, "Spatially coupled ensembles universally achieve capacity under belief propagation," *IEEE Trans. Inf. Theory*, vol. 59, no. 12, pp. 7761–7813, Dec. 2013.

[17] S. Kudekar, T. J. Richardson, and R. L. Urbanke, "Threshold saturation via spatial coupling: Why convolutional LDPC ensembles perform so well over the BEC," *IEEE Trans. Inf. Theory*, vol. 57, no. 2, pp. 803–834, Feb. 2011.

[18] A. Yedla, M. El-Khamy, J. Lee, and I. Kang, "Performance of spatially-coupled LDPC codes and threshold saturation over BICM channels," 2013, *arXiv:1303.0296*. [Online]. Available: http://arxiv.org/abs/1303.0296

[19] T. Jerkovits, G. Liva, and A. Graell i Amat, "Improving the decoding threshold of tailbiting spatially coupled LDPC codes by energy shaping," *IEEE Commun. Lett.*, vol. 22, no. 4, pp. 660–663, Apr. 2018.

[20] D. G. M. Mitchell, M. Lentmaier, and D. J. Costello, "Spatially coupled LDPC codes constructed from protographs," *IEEE Trans. Inf. Theory*, vol. 61, no. 9, pp. 4866–4889, Sep. 2015.

[21] Z. Yang, Y. Fang, G. Han, G. Cai, and F. C. M. Lau, "Design and analysis of punctured terminated spatially coupled protograph LDPC codes with small coupling lengths," *IEEE Access*, vol. 6, pp. 36723–36731, 2018.

[22] D. Truhachev, D. G. M. Mitchell, M. Lentmaier, and D. J. Costello, "Connecting spatially coupled LDPC code chains," in *Proc. IEEE Int. Conf. Commun. (ICC)*, Jun. 2012, pp. 2176–2180.

[23] D. Truhachev, D. G. M. Mitchell, M. Lentmaier, D. J. Costello, and A. Karami, "Code design based on connecting spatially coupled graph chains," *IEEE Trans. Inf. Theory*, vol. 65, no. 9, pp. 5604–5617, Sep. 2019.

[24] M. Battaglioni, A. Tasdighi, G. Cancellieri, F. Chiaraluce, and M. Baldi, "Design and analysis of time-invariant SC-LDPC convolutional codes with small constraint length," *IEEE Trans. Commun.*, vol. 66, no. 3, pp. 918–931, Mar. 2018.

[25] M. H. Tadayon, A. Tasdighi, M. Battaglioni, M. Baldi, and F. Chiaraluce, "Efficient search of compact QC-LDPC and SC-LDPC convolutional codes with large girth," *IEEE Commun. Lett.*, vol. 22, no. 6, pp. 1156–1159, Jun. 2018.

[26] S. Cammerer, V. Aref, L. Schmalen, and S. ten Brink, "Triggering wave-like convergence of tail-biting spatially coupled LDPC codes," in *Proc. Annu. Conf. Inf. Sci. Syst. (CISS)*, Mar. 2016, pp. 93–98.

[27] J. Thorpe, "Low-density parity-check (LDPC) codes constructed from protographs," *IPN Progr. Rep.*, vol. 154, pp. 1–7, Aug. 2003.

[28] Q. Chen, L. Wang, P. Chen, and G. Chen, "Optimization of component elements in integrated coding systems for green communications: A survey," *IEEE Commun. Surveys Tuts.*, vol. 21, no. 3, pp. 2977–2999, 3rd Quart., 2019.

[29] D. G. M. Mitchell, A. E. Pusane, and D. J. Costello, "Minimum distance and trapping set analysis of protograph-based LDPC convolutional codes," *IEEE Trans. Inf. Theory*, vol. 59, no. 1, pp. 254–281, Jan. 2013.

[30] V. A. Chandrasetty, S. J. Johnson, and G. Lechner, "Memory-efficient quasi-cyclic spatially coupled low-density parity-check and repeat-accumulate codes," *IET Commun.*, vol. 8, no. 17, pp. 3179–3188, Nov. 2014.

[31] S. Johnson and G. Lechner, "Spatially coupled repeat-accumulate codes," *IEEE Commun. Lett.*, vol. 17, no. 2, pp. 373–376, Feb. 2013.

[32] P. M. Olmos, D. G. M. Mitchell, D. Truhachev, and D. J. Costello, "Improving the finite-length performance of long SC-LDPC code chains by connecting consecutive chains," in *Proc. 8th Int. Symp. Turbo Codes Iterative Inf. Process. (ISTC)*, Aug. 2014, pp. 72–76.

[33] P. M. Olmos and R. L. Urbanke, "A scaling law to predict the finite-length performance of spatially-coupled LDPC codes," *IEEE Trans. Inf. Theory*, vol. 61, no. 6, pp. 3164–3184, Jun. 2015.

[34] K. Tazoe, K. Kasai, and K. Sakaniwa, "Efficient termination of spatially-coupled codes," in *Proc. IEEE Inf. Theory Workshop*, Sep. 2012, pp. 30–34.

[35] H. Niu, M. Shen, and J. A. Ritcey, "Threshold of LDPC-coded BICM for Rayleigh fading," *IEEE Commun. Lett.*, vol. 8, no. 7, pp. 455–457, Jul. 2004.

[36] S. ten Brink, G. Kramer, and A. Ashikhmin, "Design of low-density parity-check codes for modulation and detection," *IEEE Trans. Commun.*, vol. 52, no. 4, pp. 670–678, Apr. 2004.

[37] M. Stinner and P. M. Olmos, "On the waterfall performance of finite-length SC-LDPC codes constructed from protographs," *IEEE J. Sel. Areas Commun.*, vol. 34, no. 2, pp. 345–361, Feb. 2016.

[38] S. Zhang, F. Yaman, E. Mateo, T. Inoue, K. Nakamura, and Y. Inada, "Design and performance evaluation of a GMI-optimized 32QAM," in *Proc. Eur. Conf. Opt. Commun. (ECOC)*, Sep. 2017, pp. 1–3.

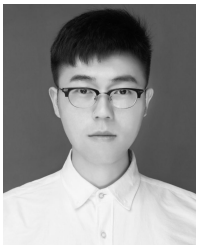

YUNLONG ZHAO received the B.Sc. degree in communication engineering from the Hunan Institute of Science and Technology, China, in 2017. He is currently pursuing the M.Sc. degree with the Department of Communication Engineering, Guangdong University of Technology, Guangzhou, China. His primary research interest is channel coding.

YI FANG (Member, IEEE) received the B.Sc. degree in electronic engineering from East China Jiaotong University, China, in 2008, and the Ph.D. degree in communication engineering from Xiamen University, China, in 2013. From May 2012 to July 2012, he was a Research Assistant of electronic and information engineering with The Hong Kong Polytechnic University, Hong Kong. From September 2012 to September 2013, he was a Visiting Scholar of electronic and electrical engineering with University College London, U.K. From February 2014 to February 2015, he was a Research Fellow with the School of Electrical and Electronic Engineering, Nanyang Technological University, Singapore. He is currently a Full Professor with the School of Information Engineering, Guangdong University of Technology, China. His current research interests include information and coding theory (especially LDPC codes), spread-spectrum modulation, and cooperative communications. He has been a Core Member of the Guangdong Innovative Research Team, since 2016. He has served as the Publicity Co-Chair for the International Symposium on Turbo Codes and Iterative Information Processing, in 2018. He has been an Associate Editor of IEEE Access, since 2018.

ZHAOJIE YANG received the B.Sc. degree in applied electronic technology from Lingnan Normal University, China, in 2016. He is currently pursuing the Ph.D. degree with the Department of Communication Engineering, Guangdong University of Technology, China. His primary research interests are channel coding and coded modulation.